Eurasian Chemical Communications

((·)) SAMI

FULL PAPER

Electronics structure and optical properties of SrPbO₃ and SrPb₀.₉₄Fe₀.₀₆O₃: A first principle approach

Unesco Chakma[a] |Ajoy Kumer[b],* | |Kamal Bikash Chakma[a] |Md. Tawhidul Islam[a] |Debashis Howlader[a] | Rasha M.K. Mohamed[c,d]

[a]*Department of Electrical and Electronics Engineering, European University of Bangladesh, Gabtoli, Dhaka-1216, Bangladesh*

[b]*Department of Chemistry, European University of Bangladesh, Dhaka-1216, Bangladesh*

[c]*Chemistry Department, Faculty of Science, Assiut University, P.O. Box: 71515, Assiut, Egypt*

[d]*Chemistry Department, College of Science, Jouf University, P.O. Box: 2014, Sakaka, Saudi Arabia*

*Corresponding Author:

Ajoy Kumer

Email: kumarajoy.cu@gmail.com

Tel.: +880 1770568699

Electronic band structures, the total density of state, the partial density of state, and optical properties were investigated using first principle method for SrPbO₃ though Generalized Gradient Approximation (GGA) based on the Perdew–Burke–Ernzerhof (PBE0). The band gap was recorded at 0.768 eV. The electron doping happens between similar electronic localized states of atoms in crystals where the section of the quality edge and electron quality of that is $\sim 10^{-2} m^2 V^{-1} s^{-1}$ with thermally activated. The density of state and partial density of state were simulated for evaluating the nature of 5s, 4d for Sr, 6s, 4f, 5d, 6p for Pb and 2s, 2p for O atom for SrPbO₃ orbital travelling with the maximum valance band (MVB) to the minimum conduction band (MCB) to explain the transition of electrons due to hybridization. The optical properties, for instance, absorption, reflection, refractive index, conductivity, dielectric function, and loss function, were calculated, which can account for the superior absorption of the visible light. The key point of this research is to determine the activity on electronics structure and optical properties for Fe doped by 6%. From the band gap and optical properties, SrPb₀.₉₄Fe₀.₀₆O₃ can give more conductivity than that of SrPbO₃, showing as a superconductor.

KEYWORDS

Band structure; density of states; doping; optical properties.

Introduction

The semiconductor device name is only insulated in a small band gap, and it can be doped with any part that changes its electronic properties in a controlled way [1]. Due to their applications in the computer and photovoltaic industry, new devices for transistors, lasers, and solar cells search for new devices, a study on advanced subject matter science [2-3]. The most commonly used semiconductor material is crystalline inorganic solid material; these materials are classified according to the phase table of their transmitted atoms and their properties. Thus, compared with silicon, compound semiconductors have both advantages and disadvantages. For example, gallium arsenide (GaAs) has six times higher electron mobility than silicon, which is capable of faster operation [4]. More significant band gaps, which allow the performance of power devices at higher temperatures, and lower temperature at low power devices at room temperature are recognized as good semiconductor [5]. Its straight band gap makes it a more favorable optoelectronic than the silicon indirect band gap [6]. It can be combined with radioactive and quadratic compositions, with regular band gap widths, allowing light emission at selected

wavelengths, and matching wavelengths with minimum reduction in optical fibers [7]. By combining multiple compounds, some semiconductor materials are tunable, for example, in the band gap or lane constant. The result is a diagonal, quadrilateral, and even curly compositions [8-9]. However, in the case of a material combination of direct and indirect band gaps, there is a ratio where the indirect band gap prevails, limiting the usability of the range for optoelectronics such as loose LEDs are limited by 660 nm [10]. The compositional polarizations of the compounds may also differ, and the explosion of the mesh against the substrate, based on the proportion of the mixture, defects to a degree depending on the imperfection. This affects the ratio of the possible radiation or sequential reconnection and determines the illumination efficiency of the device [11-12]. The transparent material is useful from light-generated wavelengths, and it can extract more effective photons from the bulk of the material [13]. That is, in such transparent materials, light yields are not only limited to the surface. The effect of the photon extraction efficiency is dependent on the index of the reference and the material.

A common term for substances that shows semiconductor properties with combinations of two or more elements as compounds remain in groups III-V or II-VI instead of simple chemicals. Gallium arsenide (GaAs) agents, and other III-V compounds (GaP, AlAs, InSb, InP, etc.) [14-16] and their mixed crystals are often used as semiconductors. It is a feature that is not available as a semiconductor such as silicon (Si) or germanium (Ge) and is used for light-emitting diode [17], semiconductor laser material [18], and microwave material [19].

On the contrary, $SrPbO_3$ exhibits a semiconducting behavior ascribed to the electropositive character of strontium and the constancy of the valence-band (VB) energy of O_2 [20]. The conductivity σ increases drastically, and an insulating-metal transition

occurs. As the doping density increases, the width of the impurity band within the gap is broadened and merges withthe conduction band (CB) [21]. Hence, the electrons are delocalized, as proven by the magnetic susceptibility and the conductivity, they become nearly temperature-independent. As carriers are introduced by Sr substitution and/or oxygen loss, the susceptibility drops, the degree of orthorhombic distortion reduces due to the decrease of the d orbital and the density of states at the Fermi level increases [22]. $SrPbO_3$ can easily lose oxygen with concomitant reduction of lead and exhibits a metal-like conductivity with a positive coefficient for the density of states, and one may expect the same origin of the conductivity as in doped specimens. The preliminary tests showed that the oxide has a high chemical inertness in basic media but dissolves in acid electrolytes; this would allow chemical analysis of divalent lead. However, superconductivity has not been observed down to 4.2 K, supporting the concept that the disproportionation of the octahedral ion is essential for the occurrence of the superconductivity. To the best of our knowledge, no studies have dealt with the PEC characterization of $SrPbO_3$. In continuation, this paper covers the complementary study of $SrPbO_3$ including the detailed data of electronic structure, optical properties, and nature of orbital. We also report, for the first time, the main features including band energy gap, ionized donor density, etc which are studied on the basis of the absorption spectra and polarization curves. It has a direct band gap (E_g) of ~1.8 eV, near to the optimum value required for the solar-energy conversion and where the losses due to absorption near the absorption edge are less pronounced. The most important key for this research is doping technology to deduce the lower band gap for soaring the adsorption of visible light while the Cu and Fe are the superior replacement due to overlapping the transition orbitals, regarding this phenomenon of dye

degradation [23]. Forouzani, M.M. *et al.* (2015) estimated that Fe and Cu atoms containing photocatalyst can show the highest activity to treatment of dye or nanoparticles that is why Fe is selected as doping materials in this study[24].

Computational methods

The theoretical calculations of semiconductor $SrPbO_3$ were simulated using first-principles calculation by the supercell approach. In Figures 1(a) and 1(b), the unit cell of $SrPbO_3$ and $SrPb_{0.94}Fe_{0.06}O_3$ in the cubic symmetry and $2 \times 1 \times 1$ supercell model considered in this study are shown. The model structure of $SrPbO_3$ and $SrPb_{0.94}Fe_{0.06}O_3$ were constructed using 33 atoms. All of the calculations in this study were performed using material studio 8.0 [25-26]. To calculate the band structure, the total density of state and partial density of state, using the method of GGA with PBE0, was optimized of CASTEP code from material studio [27]. In this condition, the band structure and density of state were calculated using the cut off at 520 eV, and k point at

$2 \times 2 \times 3$ with non-conserving pseudopotentials. The optical properties were the similar ways simulated for calculation of refractive index, reflectivity, absorption, conductivity, and loss function. Additionally, the geometric optimization was achieved, and the convergence criterion for the force between atoms was 3×10^{-6} eV/°A, the maximum displacement was 1×10^{-3}°A, and the total energy and the maximal stress were 1×10^{-5} eV/atom and 5×10^{-2} GPa, respectively.

Results and discussion

Optimized structure

The lattice parameters are a = 5.949 Å b = 6.110 Å, c = 8.470 Å and angels between them as α= 90.000 β= 90.000 A, γ= 90.000 A. The monoclinic $SrPbO_3$ crystal and also the area cluster is HermannaMauguinPnma, orthorhombic crystals system, point cluster mmm, hall -P 2ac2n, density 7.40 g/cm3 shown in Figure 1(a), and also the Fe doped optimized structure is accounted in Figure 1(b).
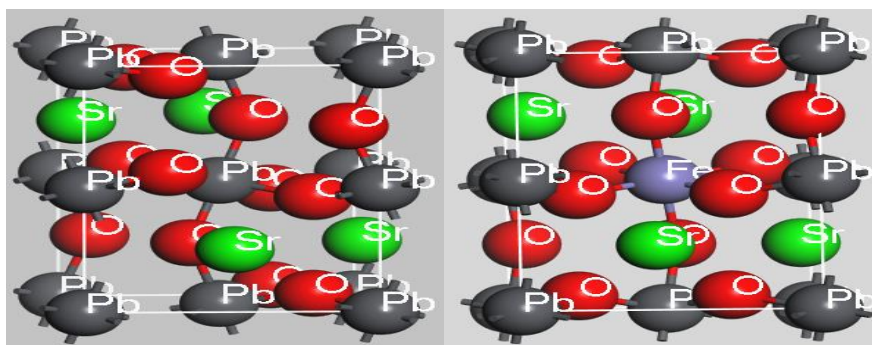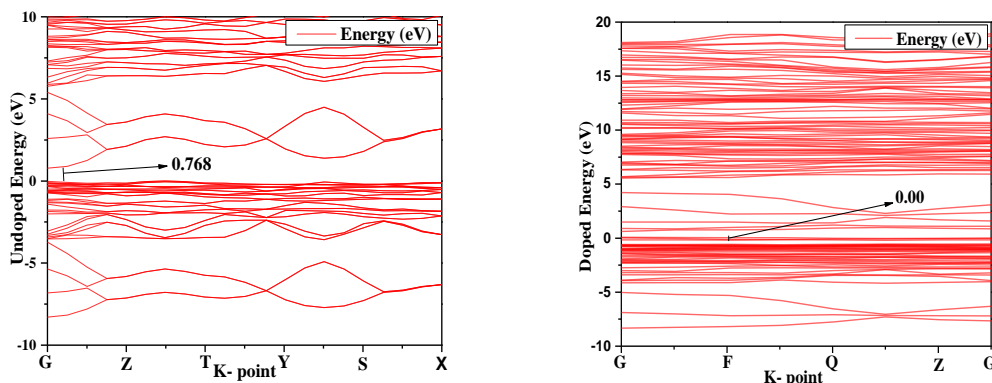

FIGURE **1**(a) Structure for SrPbO3(b)Structure for $SrPb_{0.94}Fe_{0.06}O_3$

Electronic structure

To determine the electronic band structure of $SrPbO_3$ and $SrPb_{0.94}Fe_{0.06}O_3$, the Fermi energy level was set at zero. As shown in Figure 2(a), it was absolutely found that the minimum of conduction bands (MCB) was obtained within the G symmetry point, whereas the maximum of valance bands (MVB) was connected additionally in G symmetry points. Because

each of MCB and MVB is at point G symmetry, it's known as direct band gap, and it's calculated by 0.768 eV. On one hand, according to Figure 2(a), it seems that each of higher and lower components of conduction band are well dispersed within the near G, Z, and T symmetry points than S and X symmetry point. On the other hand, the higher level of the valence band close to the G symmetry point is equally dispersive and however, lower part is

not well dispersive. In general, a lower carrier effective mass corresponds to the next carrier mobility. On the other hand, Fe doping in $SrPbO_3$ shows a different band structure whereas the minimum of conduction bands (MCB) was obtained at the F symmetry point and also the maximum of valance bands (MVB) was illustrated also in the F symmetry points. At the F symmetry point, the direct band gap is obtained by 0.00 eV.


FIGURE 2 (a) Electronic structure for $SrPbO_3$; (b) Electronic structure for $SrPb_{0.94}Fe_{0.06}O_3$

Density of states and Partial density of state

The density of the state indicates the character of electronic band structures and the splitting of an orbital. The density of states (DOS) of Sr, Pb, Fe and O atoms of $SrPbO_3$, and $SrPb_{0.94}Fe_{0.06}O_3$ crystals were calculated by PBE0 with GGA. As depicted in Figure 3, it was absolutely found that the valence bands square measure primarily was occupied by 5s, 4d for Ag, 4s 3d 4p for Fe and 4s, 3d, 4p for O atom. Meanwhile, on top of the Fermi level, the conductivity bands are composed of Ag in 5s, 4d orbital. As shown in Figure 3, the bands just below and on top of the Fermi level indicates the total density of state for undoped $SrPbO_3$. The TODS for $SrPbO_3$ is higher than doped $SrPb_{0.94}Fe_{0.06}O_3$. It is evaluated that the DOS for s, p, d, and sum of $SrPb_{0.94}Fe_{0.06}O_3$ are more delocalized than undoped $SrPbO_3$ showing in Figures 3(a), 3(b), 3(c), 3(d), 3(e), and 3(f).

(a)

(b)

(c)

(d)

(e)

(f)
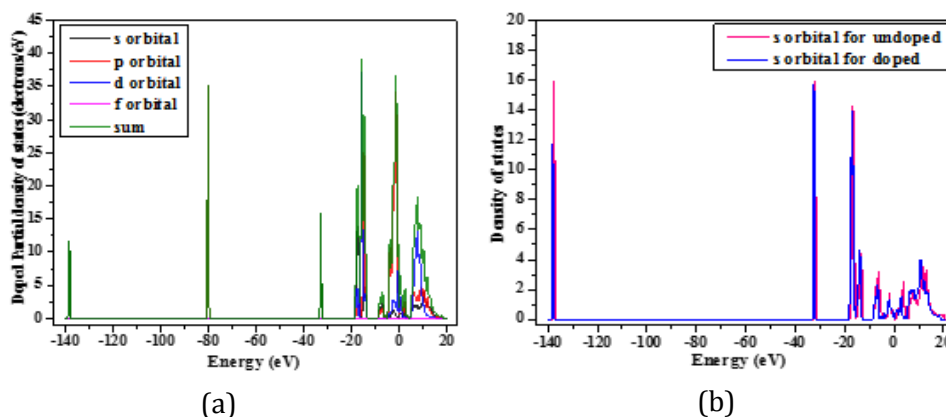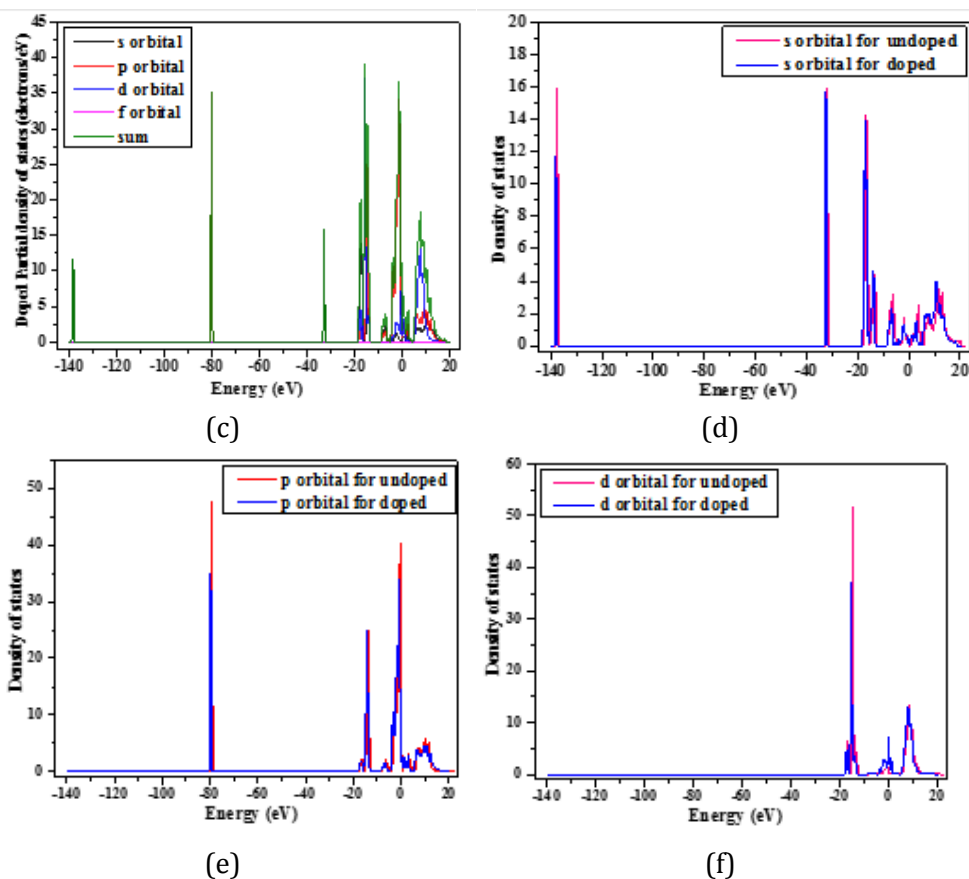
FIGURE 3 (a) comparison of total DOS for doped and undoped; (b) PDOS for undoped; (c) PDOS for doped; (d) comparison the DOS of s orbital for doped and undoped; (e) Comparison the DOS of p orbital for doped and undoped; (f) Comparison the DOS of d orbital for doped and undoped

Optical properties

Optical reflectivity

As a section of many consecutive theoretical investigations of optical phenomenon, at first, we have a tendency to go through the quantification of optical reflectivity of a crystalline material that has a major role in the electronic transition from valance band to the conduction band of compounds. The number of the wavelength is incident on the surface of the semiconductor materials that can be calculated from the reflectivity information. It's reported in a number of previous investigations that the lower reflectivity indicates the upper UV or visible light absorption [27]. In our investigation, we have a tendency to determine the reflectivity of $SrPbO_3$ and $SrPb_{0.94}Fe_{0.06}O_3$. It was found that the initial frequency was recorded around 0.35 and 5.57 severally for $SrPbO_3$. Once an ordered step-up it reached a falling down of 0.15 at 15 units and sharply accumulated at 0.22. It was fell down sharply concerning 0.02 corresponding frequencies at 23 eV as illustrated in Figure 4. In the case of $SrPb_{0.94}Fe_{0.06}O_3$, it's modified at the same point, however smaller than $SrPbO_3$. It is worth noting that the worth of reflectivity saw a dramatic zigzag between 0 to 12 eV; spectacular falling in between 12 and 25 eV and, eventually, a constant line and a constant growth up were illustrated.
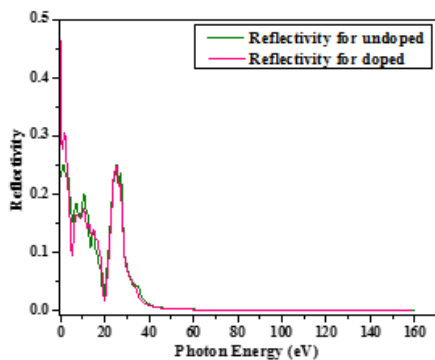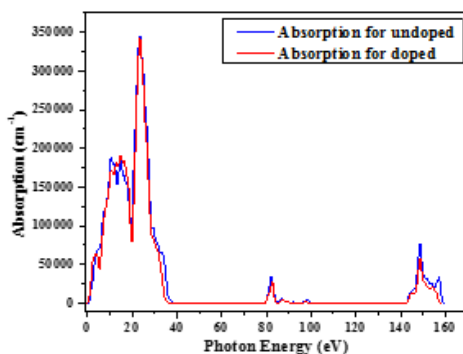
FIGURE 4 Reflectivity

FIGURE 5 Absorption

Absorption

The polycrystalline polarization technique is used to calculate the optical absorption of the $SrPbO_3$ and $SrPb_{0.94}Fe_{0.06}O_3$ materials and also, the technique includes the electrical field vector as an isotropic average over all directions. During the simulation, a small smearing value of 0.5 eV was applied in order to attain additional distinguishable absorption peaks. The obtained absorption peaks, as represented in Figure 5, are attributed to the image transition energies from the MVB to the (MCB) underneath visible light irradiation, which indicates that this material can absorb photons of visible range. Each of $SrPbO_3$ and $SrPb_{0.94}Fe_{0.06}O_3$ shows the modification at the same point, but $SrPb_{0.94}Fe_{0.06}O_3$ is slightly higher than $SrPbO_3$.

Refractive index

The index of refraction of a material is an impactful parameter for mensuration of the photon absorbed throughout the method of chemical degradation from the solutions. The Large value of the index of refraction is related to the larger and denser medium, corresponding to a very previous investigation. Figure 6 displays the refraction index as a function of photon energy wherever the real part and, therefore, the imaginary part of a complex number for each of the undoped and doped are mentioned, showing an inverse pattern. At the initial point of photon energy, the refraction index is higher for the real part while the imaginary part of a complex number is nearly closed to zero. Subsequently, a decrease of each element encounters them to each other for doped and undoped to 23 eV with a value of 0.6, and afterward, they follow a constant pattern with slightly totally different values of refraction index and the same for each undoped and doped of $SrPbO_3$.

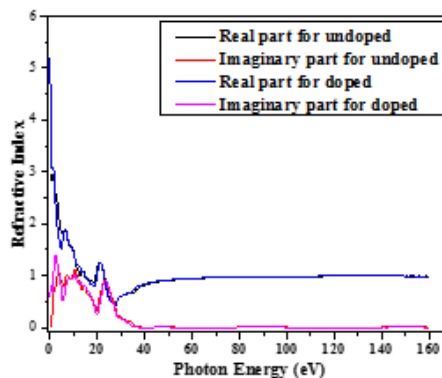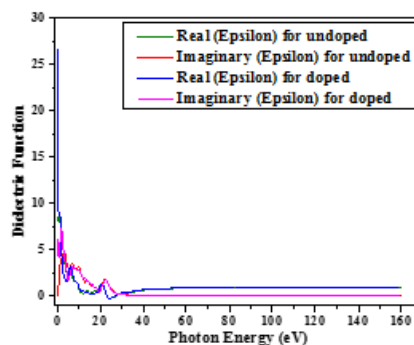**FIGURE 6** Refractive index

FIGURE 7 Dielectric function

Dielectric function

The dielectric function is an incredibly necessary tool to analyze the optical properties that are expounded with sorption properties as the following equation for solid.

$$\varepsilon = \varepsilon_1(\omega) + i\varepsilon_2(\omega)$$

Here, $\varepsilon_1(\omega)$ and $\varepsilon_2(\omega)$ denote nonconductor constant (real part) and the dielectric loss factor (imaginary part) respectively. Nonconductor function includes a relationship with the space of materials that are physically equivalent to the permittivity or absolute permittivity. The real part of the dielectric function represents the energy storage capability in the electric field, and also the pure imaginary number represents the energy dissipation capability of the nonc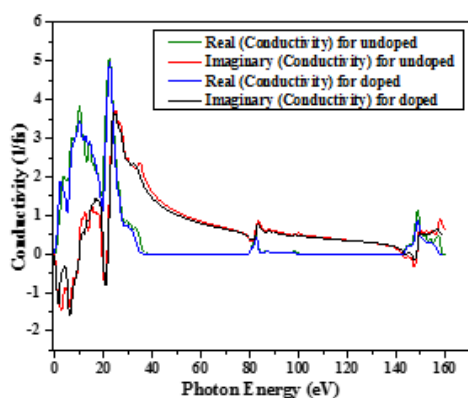onductor materials. According to Figure 7, the imaginary part number is a smaller amount than the real part from 0 eV to 5 eV frequencies. However, from 6 eV to 16 eV, the imaginary part is larger than real part, showing the same real and imaginary part for the doped and undoped $SrPbO_3$.

Conductivity

The physical phenomenon of the semiconductor on the basis of the energy band and orbital electrons is joined with the discrete parts of electrons in orbit. This can be conjointly made due to the presence of holes and free electrons within the crystal molecules. According to Figure 8, the physical phenomenon of $SrPb_{0.94}Fe_{0.06}O_3$ is slightly larger than $SrPbO_3$ within both cases.
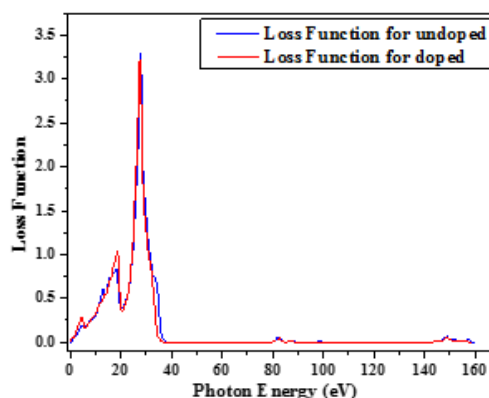

FIGURE 8 Conductivity

FIGURE 9 Loss function

Loss function

There are two regions for the electronic energy loss function, including high energy region or low energy region for optical properties. The primary region is that the higher loss function indicates the higher energy region with modification of frequency or spectra. The alternative is the low energy loss function, together with the energy less than one that will give info regarding composition and electronic structure. The energy loss function for optical properties is connected to the insulator constant of the materials among the variety of validity of the dielectric function. As shown in Figure 9, the loss function for $SrPb_{0.94}Fe_{0.06}O_3$ is poor higher than $SrPbO_3$

Conclusion

In our simulation, we had used the generalized gradient approximation (GGA) on the Perdew–Burke–Ernzerhoff (PBE0) within the strategy to check the electronic structures of $SrPbO_3$ and $SrPb_{0.94}Fe_{0.06}O_3$ crystals. From the electronic structure, the band gap was illustrated by Fedoping substitution Pb, and the delocalization was also enlarged. On the other hand, a doping activity on $SrPbO_3$ for the

optical properties was calculable, illustrating nearly higher than undoped $SrPbO_3$. To sum up, when doping Feby6%, the $SrPbO_3$ almost acts as a superconductor.

Orcid:

Ajoy Kumer: https://orcid.org/0000-0001-5136-6166

References

[1] E.F. Schubert, *Journal of Vacuum Science & Technology A: Vacuum, Surfaces, and Films.,* **1990**, *8*, 2980-2996.

[2] M. Bosi, C. Pelosi, *Progress in Photovoltaics: Research and Applications,* **2007**, *15*, 51-68.

[3] K. Nomura, H. Ohta, A. Takagi, T. Kamiya, M. Hirano, H. Hosono, *Nature,* **2004**, *432*, 488-492.

[4] R.K. Willardson, *Journal of Applied Physics.,* **1959**, *30*, 1158-1165.

[5] M. Saba, C. Ciuti, J. Bloch, V. Thierry-Mieg, R. André, Le Si Dang, S. Kundermann, A. Mura, G. Bongiovanni, J.L. Staehli, B. Deveaud, *Nature,* **2001**, *414*, 731 -735.

[6] G. Dennis, Hall, MRS Online Proceedings Library Archive, **1993**, 298, 367-378.

[7] M. Centini, C. Sibilia, M. Scalora, G.D. Aguanno, M. Bertolotti, M.J. Bloemer, C.M. Bowden, I. Nefedov, *Physical Review E.,* **1999**, *60*, 4891-4898.

[8] G. Antonini, A. Orlandi, A.E. Ruehli, *IEEE transactions on electromagnetic compatibility,* **2002**, *44*, 399-403.

[9] P. Bettini, F. Trevisan, A. Formisano, *IEEE transactions on magnetics*, **2002**, *38*, 1089-1092

[10] F.G. Kellert, R.L. Moon, *Journal of electronic materials,* **1986**, *15*, 13-19.

[11] D. Wood, J. Tauc, *Physical Review B.,* **1972**, *5*, 3144- 3151.

[12] J. Simon, V. Protasenko, C. Lian, H. Xing, D. Jena, *Science,* **2010**, *327*, 60-64.

[13] Wu Chi, *Emerging Components and Technologies for All-Optical Photonic Systems II.,* **1997**, *2918*, 14-25.

[14] S.M. Ku, *Journal of the Electrochemical Society,* **1966**, *113*, 813 -816.

[15] S. Adachi, C.W. Tu, *Physics Today*, **1994**, *47*, 99-100.

[16] A.H. Reshak, *The Journal of Chemical Physics*, **2006**, *125*, 034710.

[17] S.I. Tsintzos, N.T. Pelekanos, G. Konstantinidis, Z. Hatzopoulos, P.G. Savvidis, *Nature,* **2008**, *453*, 372- 375.

[18] J. Chilla, S. Butterworth,A. Zeitschel, J. Charles, A. Caprara, M.K. Reed, L.A. Spinelli, *Solid State Lasers XIII: Technology and Devices.,* **2004**, *5332*, 143-150.

[19] A.M. Morales, C.M. Lieber, *Science,* **1998**, *279*, 208-211.

[20] B. Hadjarab, A. Bouguelia, M. Kadi-Hanifi, M. Trari, *Journal of Physics: Condensed Matter.,* **2006**, *18*, 8551 -8561.

[21] K.C. Mishra, K.H. Johnson, P.C. Schmidt, *Physical Review B.,* **1995**, *51*, 13972- 13976.

[22] D.D. Kleppinger, F.A. Lindholm,*Solid-State Electronics.,* **1971**, *14*, 407-416.

[23] H.R. Mardani, M. Forouzani, M. Ziari, P. Biparva, *Spectrochimica Acta Part A: Molecular and Biomolecular Spectroscopy,* **2015**, *141*, 27-33.

[24] M. Forouzani, H.R. Mardani, M. Ziari, A. Malekzadeh, P. Biparva, *Chemical Engineering Journal.,* **2015**, *275*, 220-226.

[25] U.K Chowdhury, M.A. Rahman, M.A. Rahman, M.T.H. Bhuiyan, M.L. Ali, *Cogent Physics.,* **2016**, *3*, 1231361.

[26] M.D. Segall, P.J.D. Lindan, M.J. Probert, C.J. Pickard, P.J. Hasnip, S.J. Clark, M.C. Payne, *Journal of Physics: Condensed Matter.,* **2002**, *14*, 2717-2744.

[27] P.J. Perdew, K. Burke, M. Ernzerhof, *Physical Review Letters,* **1996**, *77*, 3865-3868.